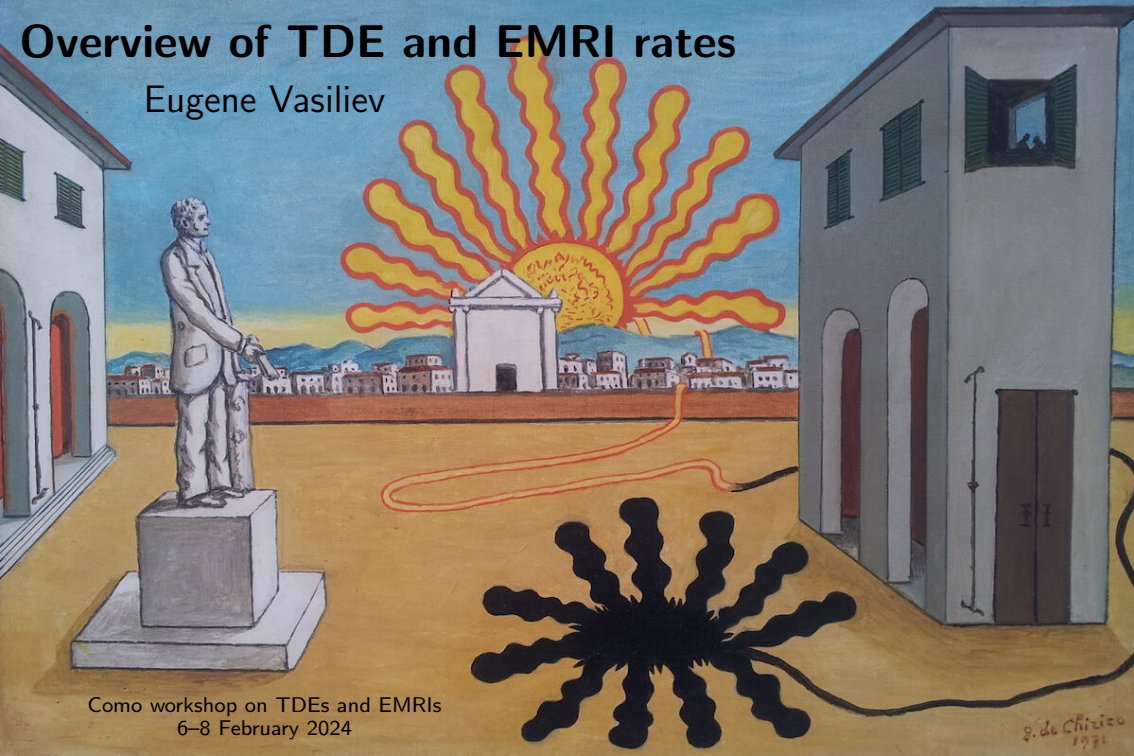


Overview of TDE and EMRI rates

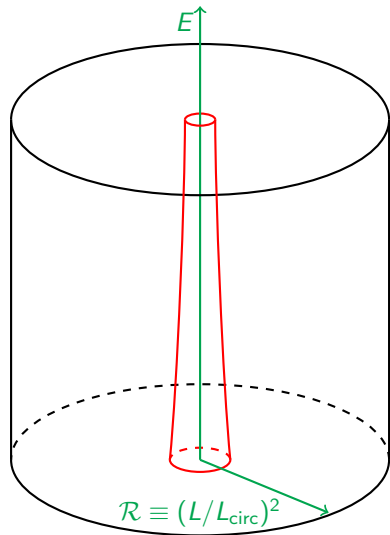
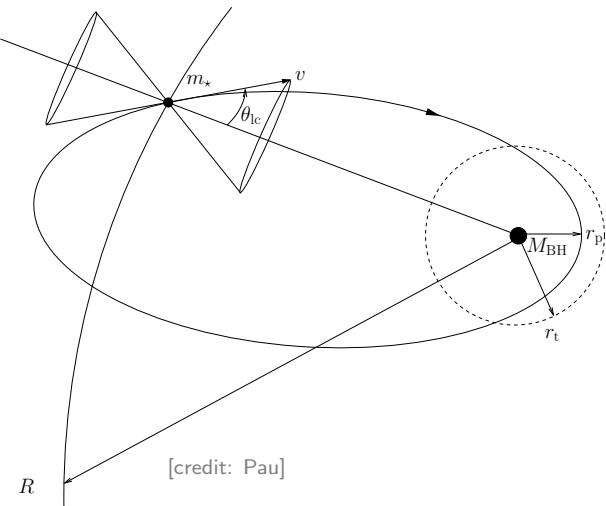
Eugene Vasiliev



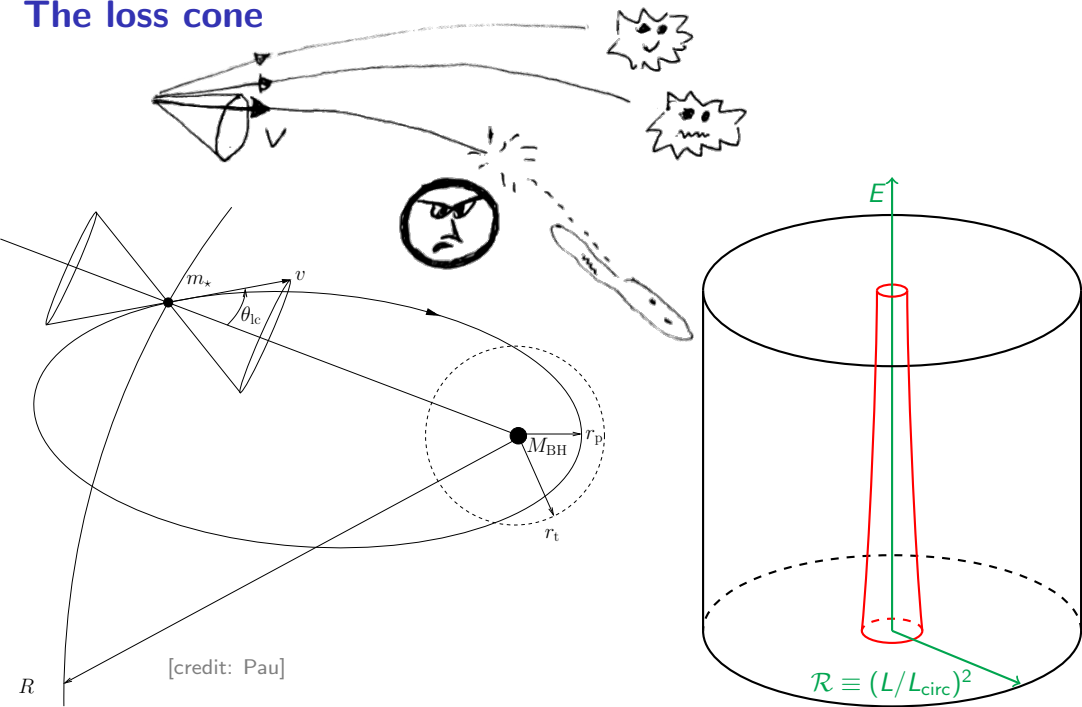
Como workshop on TDEs and EMRIs
6–8 February 2024

G. de Chizico
1971

The loss cone



The loss cone



Orbits intro

Keplerian orbit with semimajor axis a and eccentricity e :

$$E = -\frac{GM_{\bullet}}{2a}$$

$$T_{\text{orb}} = \frac{2\pi a^{3/2}}{\sqrt{GM_{\bullet}}}$$

$$L_{\text{circ}} = \frac{GM_{\bullet}}{\sqrt{-2E}} = \sqrt{GM_{\bullet}a}$$

$$L = L_{\text{circ}} \sqrt{1 - e^2}$$

$$\mathcal{R} \equiv (L/L_{\text{circ}})^2 = 1 - e^2 \approx 2(1 - e) \text{ for very eccentric orbits}$$

If the physical radius of the loss cone $r_{\text{LC}} \ll a$, only stars with $1 - e \ll 1$ are able to enter it, and in this case $L_{\text{LC}} \approx \sqrt{2GM_{\bullet}r_{\text{LC}}}$.

Distribution functions intro

$f(\mathbf{x}, \mathbf{v})$ is the DF in the 6d phase space (normalized so that $\int f d^3\mathbf{x} d^3\mathbf{v} = N_* m_*$) according to Jeans' theorem, in a steady state it may depend only on the integrals of motion, i.e., in a spherical potential, $f(E, L)$ or $f(E, \mathcal{R})$.

The mass of stars per unit E, \mathcal{R} is

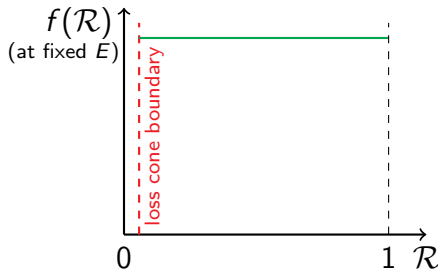
$$N(E, \mathcal{R}) dE d\mathcal{R} = g(E, \mathcal{R}) f(E, \mathcal{R}) dE d\mathcal{R},$$

where the density of states $g(E, \mathcal{R}) = 4\pi^2 T_{\text{orb}}(E, \mathcal{R}) L_{\text{circ}}^2(E) \approx g(E)$;

in the Keplerian case, $g(E) = \frac{\sqrt{2} \pi^3 (GM_\bullet)^3}{(-E)^{5/2}}$.

In case of isotropic velocity distribution (\Leftrightarrow "thermal" eccentricity distribution), $f(E, \mathcal{R}) = f(E)$.

Such a distribution is thermodynamically preferred, but cannot be fully achieved because of the existence of the loss cone.



Relaxation intro

Classical ("Chandrasekhar") two-body relaxation theory:
under the assumptions of

1. uncorrelated pairwise encounters,
2. weak deflections (impact parameter $b \gg b_{90} \equiv Gm_*/v^2$),
3. slow evolution ($T_{\text{orb}} \ll T_{\text{rel}}$),

the evolution of the DF $f(E, \mathcal{R})$ can be described by
the orbit-averaged Fokker-Planck equation:

$$\frac{\partial [f(E, \mathcal{R}, t) g(E, \mathcal{R})]}{\partial t} = - \frac{\partial \mathcal{F}_E(E, \mathcal{R}, t)}{\partial E} - \frac{\partial \mathcal{F}_R(E, \mathcal{R}, t)}{\partial \mathcal{R}}$$
$$\left. \begin{aligned} - \mathcal{F}_E &= \mathcal{D}_{EE} \frac{\partial f}{\partial E} + \mathcal{D}_{ER} \frac{\partial f}{\partial \mathcal{R}} + m_* \mathcal{A}_E f \\ - \mathcal{F}_R &= \mathcal{D}_{RE} \frac{\partial f}{\partial E} + \mathcal{D}_{RR} \frac{\partial f}{\partial \mathcal{R}} + m_* \mathcal{A}_R f \end{aligned} \right\} \text{fluxes in } E \text{ and } \mathcal{R}$$

diffusion coefficients stellar mass advection coefficients

Relaxation intro (cont.)

Advection and diffusion coefficients are given by some integrals over the DF of *field* stars, and nearly always this field DF is approximated by the isotropized form $\bar{f}(E) \equiv \int_0^1 f(E, \mathcal{R}) d\mathcal{R}$:

$$\mathcal{D}_{EE}(E, \mathcal{R}) = m_{\star} \int dE' \bar{f}(E') K(E', E, \mathcal{R}) \quad \text{with some kernel } K.$$

Usually the field DF is the same as the test stars' DF evolving under the Fokker–Planck eqn.

In the multi-mass case (e.g., $1 M_{\odot}$ stars and $10 M_{\odot}$ black holes), diffusion coefficients are the same for all species, and the field DF is given by the sum of all species' DFs *additionally weighted by field stars' mass*, i.e.,

$$\mathcal{D}_{EE}(E, \mathcal{R}) = \sum_i m_{\star,i} \int dE' \bar{f}_i(E') K(E', E, \mathcal{R}).$$

Thus the relaxation rate is often dominated by the most massive species.

OTOH the advection coefficients are not weighted by the field star masses,

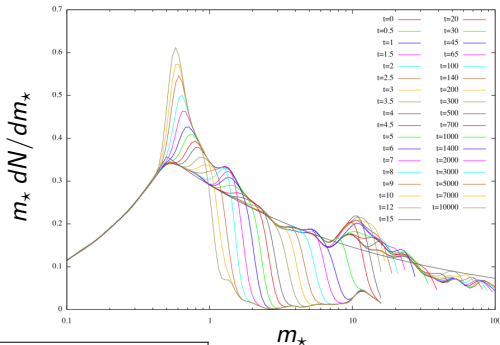
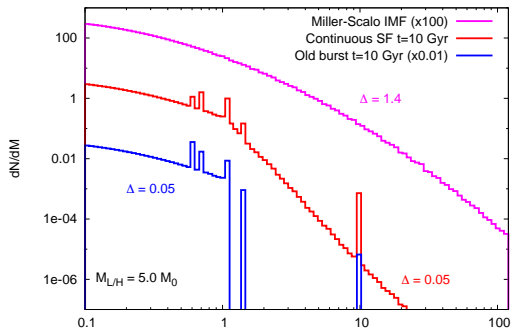
$$\mathcal{A}_E = \sum_i \int dE' \bar{f}_i(E') \mathcal{X}(E', E, \mathcal{R}),$$

but then additionally multiplied by the test star mass in the eqn for flux.

This is what gives rise to dynamical friction and mass segregation.

Relaxation in multimass systems

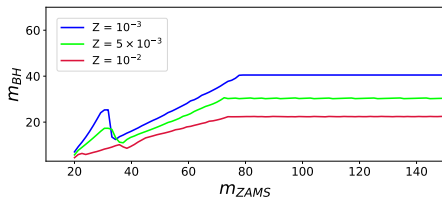
For a typical IMF, a few % of mass is contained in black holes with $m_{\star} \gtrsim 10 M_{\odot}$: this means that they significantly contribute to the relaxation rate even without mass segregation!



[Alexander & Hopman 2009] $M [M_{\odot}]$

see also

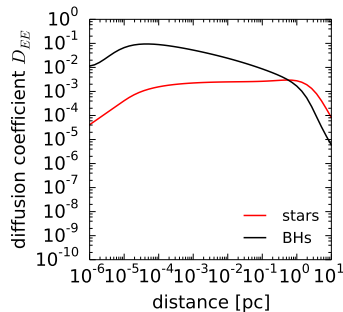
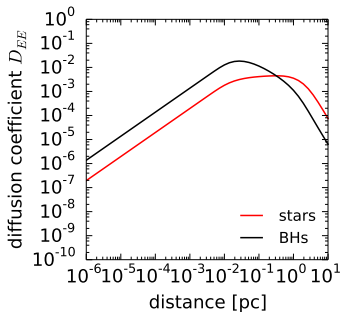
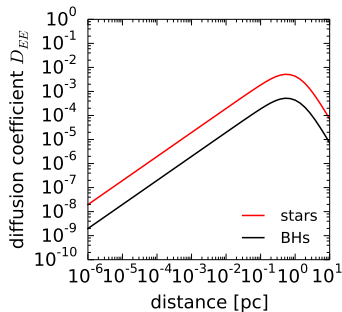
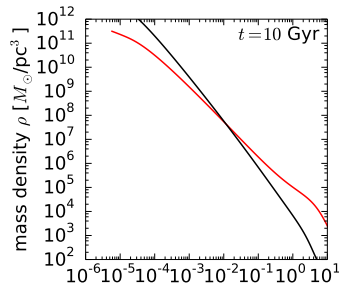
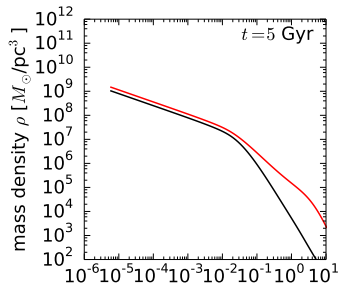
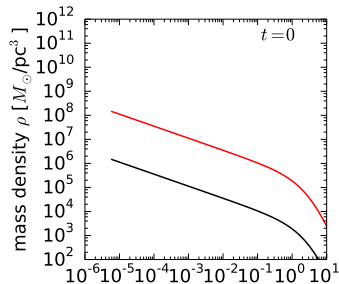
Preto & Amaro-Seoane 2010,
 Stone & Metzger 2016,
 Bortolas 2022, ...



low-metallicity stars
 produce heavier BHs

Diffusion in energy and mass segregation

example of re-growth of the Bahcall–Wolf cusp



Diffusion in angular momentum

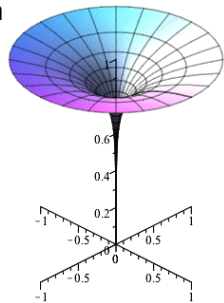
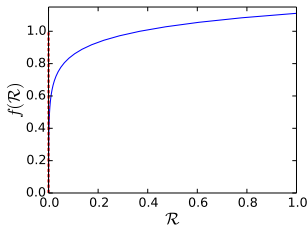
If we ignore for the moment the diffusion in the energy direction, the 1d Fokker–Planck equation for $f(\mathcal{R}, t)|_{E=\text{const}}$ is

$$\frac{\partial f(\mathcal{R}, t)}{\partial t} = -\frac{\partial \mathcal{F}_{\mathcal{R}}(\mathcal{R}, t)}{\partial \mathcal{R}}, \quad -\mathcal{F}_{\mathcal{R}} = \mathcal{D}_{\mathcal{R}\mathcal{R}} \frac{\partial f}{\partial \mathcal{R}} + m_{\star} \mathcal{A}_{\mathcal{R}} f$$

The advection (drift) coefficient $\mathcal{A}_{\mathcal{R}}$ turns out to be zero (because the flux should vanish for the isotropic DF $f(\mathcal{R}) = \text{const}$), and the diffusion coefficient, to first order, is $\mathcal{D}_{\mathcal{R}\mathcal{R}}(E, \mathcal{R}) \approx \mathcal{D}(E) \mathcal{R}$.

This is equivalent to the diffusion or heat conduction equation in the cylindrical geometry, and the steady-state solution is

$$0 = \mathcal{D} \frac{\partial}{\partial \mathcal{R}} \left(\mathcal{R} \frac{\partial f}{\partial \mathcal{R}} \right) \implies f(\mathcal{R}) = \frac{\bar{f} \ln[\mathcal{R}/\mathcal{R}_{\text{LC}}]}{\ln[1/\mathcal{R}_{\text{LC}}] - 1 + \mathcal{R}_{\text{LC}}}.$$



Empty vs. full loss cone regimes

recall that stars are captured (loss cone is purged) only at pericentre passages

Two regimes:

compare T_{orb} with the loss cone repopulation timescale

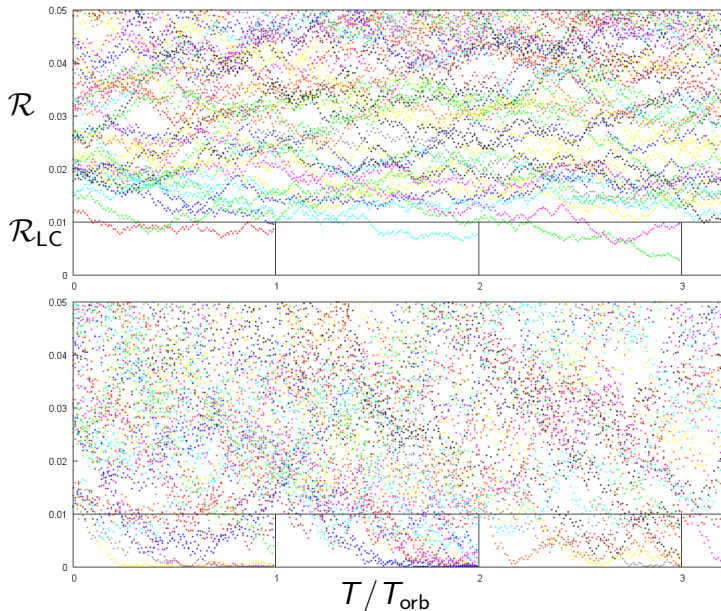
$$\sqrt{\mathcal{D}_{\mathcal{R}\mathcal{R}} T_{\text{rep}}} \simeq R_{\text{LC}}.$$

$$q \equiv \frac{T_{\text{orb}}}{T_{\text{rep}}} = \frac{\mathcal{D} T_{\text{orb}}}{R_{\text{LC}}}.$$

$q \ll 1$: empty loss cone

$q \gg 1$: full loss cone

[Cohn & Kulsrud 1978]



Empty vs. full loss cone regimes

When the loss cone is not entirely empty, the DF at its boundary is > 0 ; one can write the boundary condition in the form

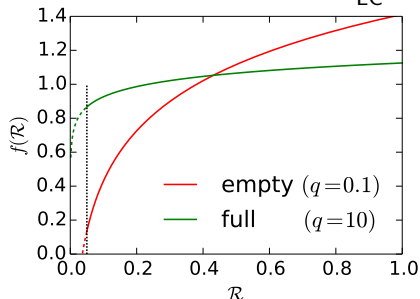
$$0 = f(\mathcal{R}_{\text{LC}}) - \alpha \mathcal{R} \left. \frac{\partial f(\mathcal{R})}{\partial \mathcal{R}} \right|_{\mathcal{R}_{\text{LC}}}, \quad \text{where } \alpha \approx (q^2 + q^4)^{1/4} \text{ and } q = \frac{\mathcal{D} T_{\text{orb}}}{R_{\text{LC}}}.$$

The steady-state solution is

$$f(\mathcal{R}) = \frac{\bar{f} (\ln[\mathcal{R}/\mathcal{R}_{\text{LC}}] + \alpha)}{\ln[1/\mathcal{R}_{\text{LC}}] + (1 - \mathcal{R}_{\text{LC}})(\alpha - 1)},$$

and the flux into the loss cone is

$$-\mathcal{F}_{\mathcal{R}} = \frac{\bar{f} \mathcal{D}}{\ln[1/\mathcal{R}_{\text{LC}}] + (1 - \mathcal{R}_{\text{LC}})(\alpha - 1)}.$$

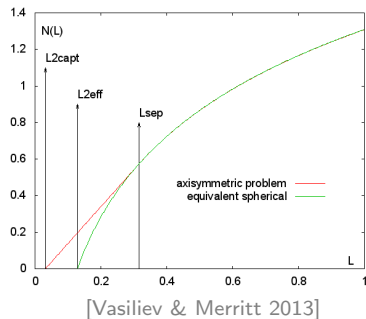
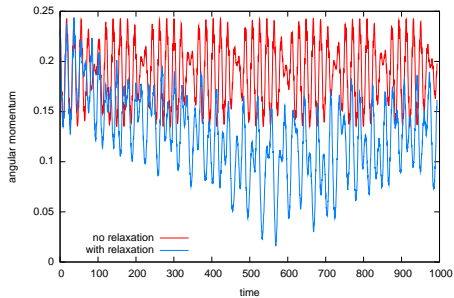
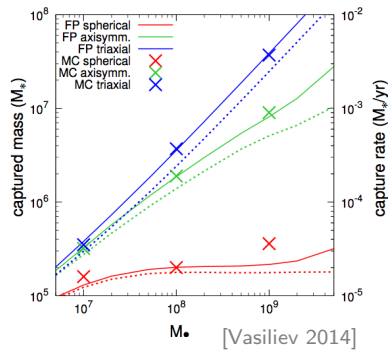


In the empty LC regime, the flux is proportional to the relaxation rate \mathcal{D} and only logarithmically depends on the loss-cone size \mathcal{R}_{LC} , while in the full LC regime the flux is linearly proportional to \mathcal{R}_{LC} and nearly independent of the relaxation rate.

Complication #1: non-spherical galaxy potentials

Even if the black hole dominates the total potential, a non-spherical stellar distribution produces torques that lead to periodic variations of orbital angular momentum even in absence of relaxation.

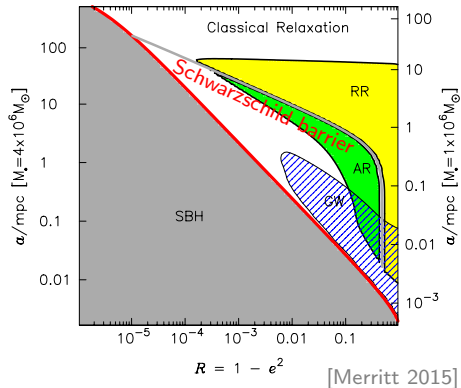
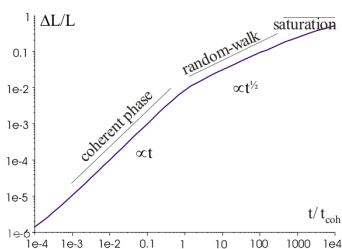
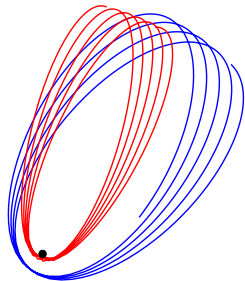
Stars from the "centrophilic" orbits can sustain much higher capture rates than in spherical galaxies *if the relaxation rate is low*, and when they are drained, the capture rates are only moderately higher due to log-dependence of flux on \mathcal{R}_{LC} .



Complication #2: resonant relaxation

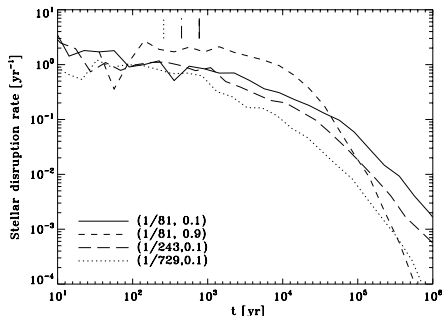
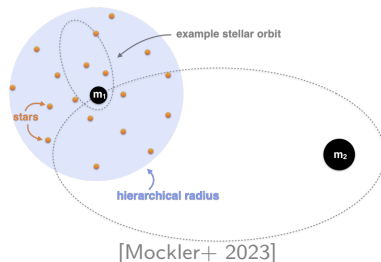
In a [nearly-]Keplerian potential, orbits are almost closed ellipses and can interact with each other over many periods before "decorrelating" due to orbit precession.

This gives rise to enhanced relaxation in angular momentum [Rauch & Tremaine 1996; Hopman & Alexander 2006], but only at eccentricities below the "Schwarzschild barrier" set by relativistic precession [Merritt+ 2011; Brem+ 2013; Hamers+ 2014; Bar-Or & Alexander 2015].

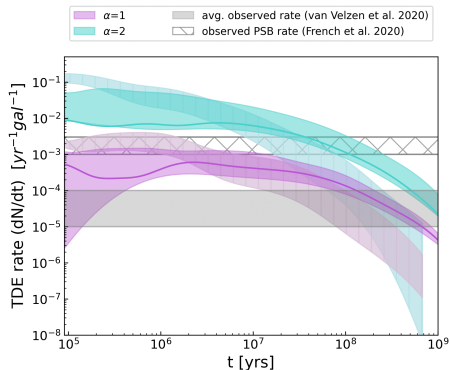


Complication #3: binary SMBH and the Kozai–Lidov effect

Short-term boost in TDE rates after the formation of a binary SMBH, and longer-term enhancement in rates due to KL oscillations (periodic variations of angular momentum) [Ivanov+ 2005; Chen+ 2008–2011; Wegg & Bode 2011; Li+ 2017; Darbha+ 2018; Thorp+ 2019; Lezhnin & Vasiliev 2019; Naoz+ 2022; Melchor+ 2023]



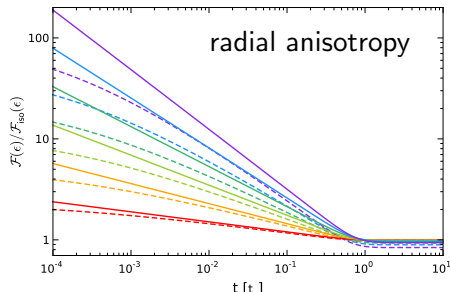
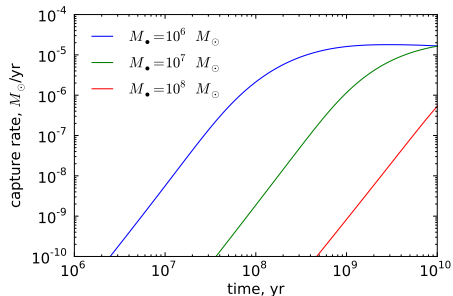
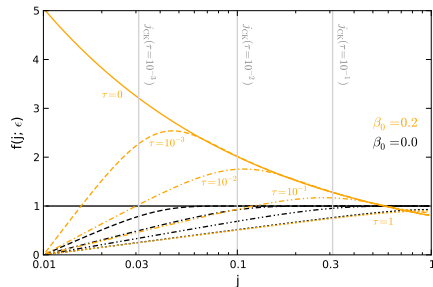
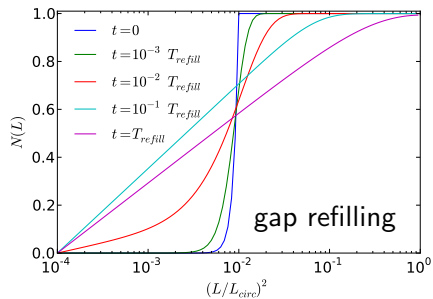
[Chen+ 2009]



[Melchor+ 2023]

Complication #4: anisotropic and time-dependent loss cones

steady-state log profile $f(\mathcal{R})$ is established only after [a fraction of] T_{rel}

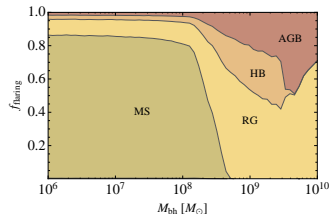
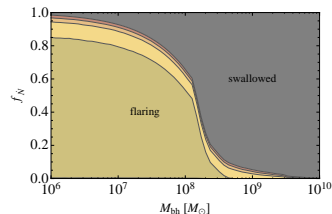
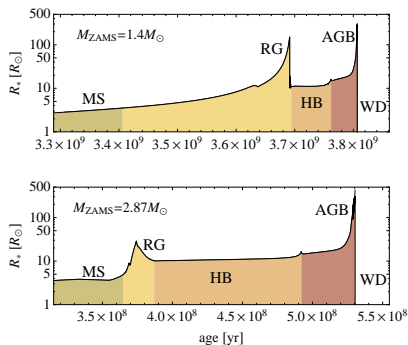


Complication #5: giant stars and partial disruptions

Since the tidal radius is $r_{\text{LC}} \simeq r_{\star} (M_{\bullet}/m_{\star})^{1/3}$, giant stars can have a significant contribution to the total TDE rate [Magorrian & Tremaine 1999, McLeod+ 2012]. Stars can "grow" into the loss cone even without changing their orbit [Syer & Ulmer 1999], and the outer envelope of a giant can be repeatedly stripped in many partial disruption flares [McLeod+ 2013].

For $M_{\bullet} \gtrsim 10^8 M_{\odot}$, r_{LC} for main-sequence stars is below r_{Schw} , so only giants produce TDE flares.

Partial TDEs can be much more frequent than "normal" ones, "steal" some fraction of the latter, and even lead to ejection of the remnant [Bortolas+ 2023].



[McLeod+ 2012]

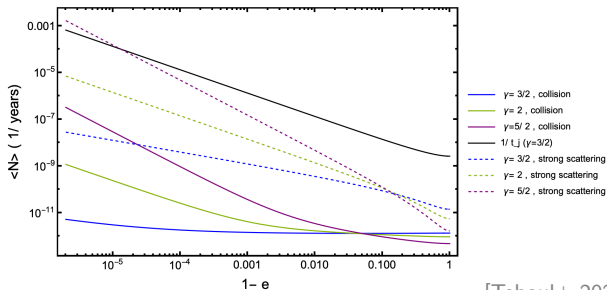
Complication #6: strong scattering and stellar collisions

Physical collisions mostly relevant for giant stars and can make them "invisible", though rarely destroy the stars entirely [Dale+ 2009; Amaro-Seoane & Chen 2014, ...]

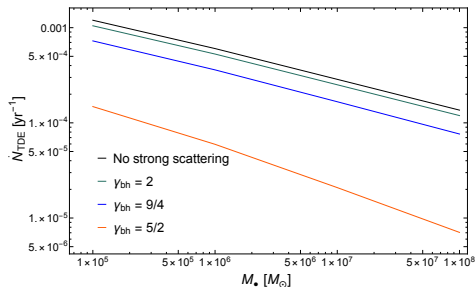
Strong scattering events (large-angle deflections) are "rare" (fraction $\propto 1/\ln \Lambda$ of all two-body encounters), and violate the local diffusion approximation.

Rarely considered in the context of Fokker-Planck or Monte Carlo methods

[Goodman 1983 (unpublished thesis); Fregeau & Rasio 2004; Bar-Or+ 2013; Teboul+ 2023]

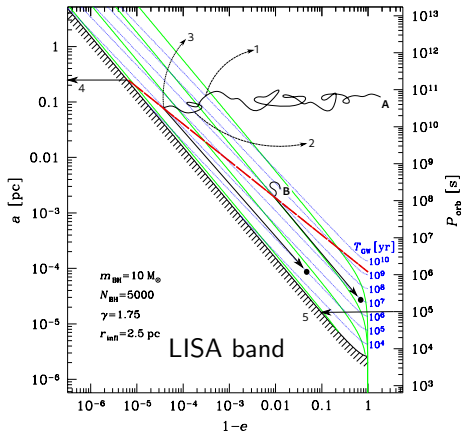
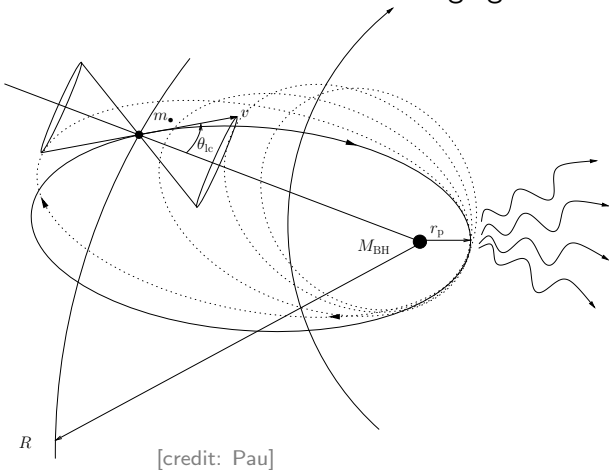


[Teboul+ 2023]



Tidal disruptions vs. EMRIs

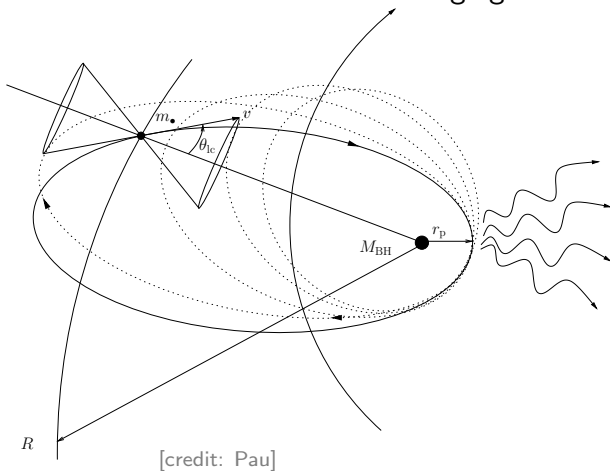
Compact objects (NS, BH) are not tidally disrupted, but can lose enough energy to gravitational waves during close pericentre passages to end up on very tight orbits (hence in the LISA frequency band), possibly completing hundreds of orbits before merging.



[2011.03059]

Tidal disruptions vs. EMRIs

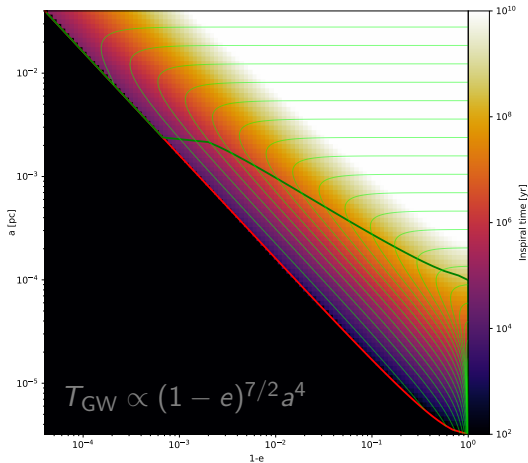
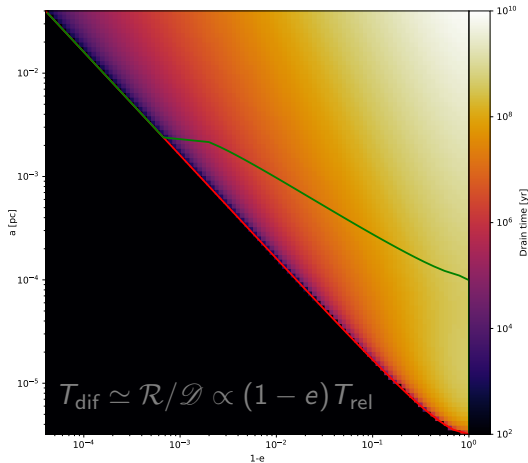
Compact objects (NS, BH) are not tidally disrupted, but can lose enough energy to gravitational waves during close pericentre passages to end up on very tight orbits (hence in the LISA frequency band), possibly completing hundreds of orbits before merging.



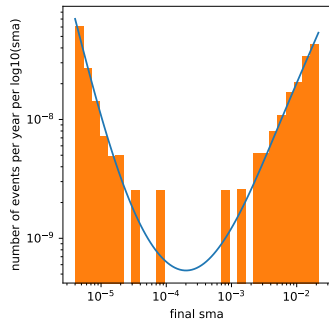
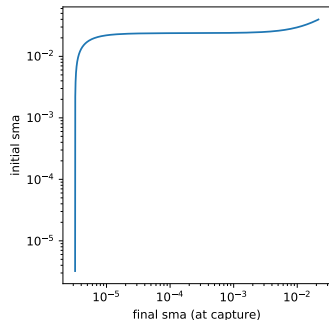
Formation of EMRIs

In the standard scenario, COs diffuse through phase space just like stars, but when they reach high enough eccentricity that the GW emission timescale T_{GW} becomes shorter than the diffusion timescale, they slide down towards small a and low e .

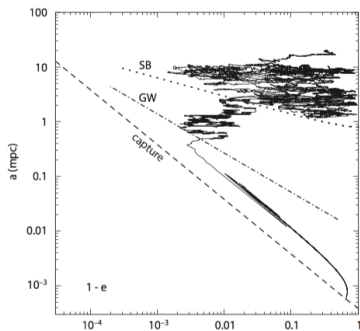
The division line $T_{\text{GW}} = T_{\text{dif}}$ crosses the loss-cone boundary at some a_{GW} .



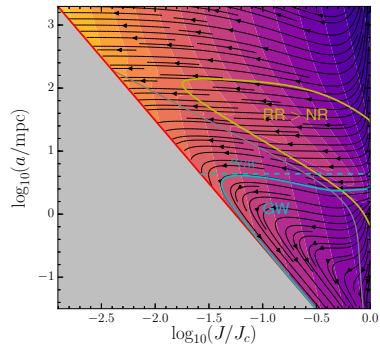
Formation of EMRIs



Resonant relaxation was once thought to be a significant factor affecting the EMRI rates, but more careful analysis showed that it is likely unimportant in the region of interest [cf. Alexander 2017]: the GW onset occurs to the left of the Schwarzschild barrier, and hence still determined by ordinary two-body relaxation.



[Merritt+ 2010]



[Bar-Or & Alexander 2015]

Methods for computing TDE rates

Steady-state

- ▶ Cohn & Kulsrud (1978) approximation in the two asymptotic regimes (empty and full LC) [e.g., Zhong+ 2023]
- ▶ "Standard approach": integrate the CK78 steady-state flux from 1d FP in angular momentum over the entire range of energies, weighted by $f(E)$ [e.g., Magorrian & Tremaine 1999; Wang & Merritt 2004; Merritt 2010; Stone & Metzger 2016]

Methods for computing TDE rates

Steady-state

- ▶ Cohn & Kulsrud (1978) approximation in the two asymptotic regimes (empty and full LC) [e.g., Zhong+ 2023]
- ▶ "Standard approach": integrate the CK78 steady-state flux from 1d FP in angular momentum over the entire range of energies, weighted by $f(E)$ [e.g., Magorrian & Tremaine 1999; Wang & Merritt 2004; Merritt 2010; Stone & Metzger 2016]

Time-dependent (DF and/or potential)

- ▶ Same CK78 flux in angular momentum, but for an evolving $f(E, t)$ described by the 1d FP in energy space [e.g., Murphy+ 1991; Hopman & Alexander 2006; Amaro-Seoane & Preto 2009; Merritt 2010]; PHASEFLOW [Vasiliev 2017; Pfister+ 2019, 2020; Bortolas+ 2022, 2023]
- ▶ Full 2d FP in the $\{E, L\}$ space [Cohn & Kulsrud 1978; Vasiliev & Zelnikov 2008; Merritt 2015; Pan & Yang 2021; Broggi+ 2022]
- ▶ Monte Carlo in the $\{E, L\}$ space [Shapiro & Marchant 1978; Freitag & Bentz 2002; Hopman 2009; Vasiliev 2015; Fragione & Sari 2018; Zhang & Amaro-Seoane 2023]
- ▶ Stellar-dynamical fluid models [Amaro-Seoane & Spurzem 2001]
- ▶ N -body simulations [Preto & Amaro-Seoane 2010; Zhong+ 2014; Panamarev+ 2019; ...]

Methods (cont.)

Monte Carlo

- ▶ Follows the same Chandrasekhar prescription for two-body relaxation as FP
- ▶ Can incorporate additional physics more easily (stellar binaries, stellar evolution, non-sphericity, large kicks, GW emission, ...)
- ▶ More "noisy" than FP (but still can use $N_{\text{body}} \simeq N_{\star}$ and a realistic r_{LC})

Methods (cont.)

Monte Carlo

- ▶ Follows the same Chandrasekhar prescription for two-body relaxation as FP
- ▶ Can incorporate additional physics more easily (stellar binaries, stellar evolution, non-sphericity, large kicks, GW emission, ...)
- ▶ More "noisy" than FP (but still can use $N_{\text{body}} \simeq N_{\star}$ and a realistic r_{LC})

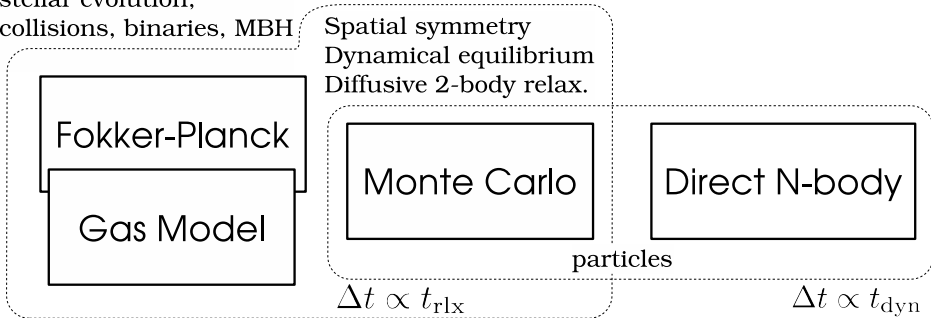
N-body

- ▶ "Free" from approximations regarding relaxation and geometry
- ▶ Much more expensive even on modern hardware
- ▶ Can rarely be run with $N_{\text{body}} = N_{\star}$ and realistically small $r_{\text{LC}} \implies$ need to determine scaling relations and extrapolate to real galaxies

Numerical methods for collisional stellar dynamics

Highly approximate **Physical realism** “exact”
→

Simplified MF,
stellar evolution,
collisions, binaries, MBH



T_{CPU} for
core-collapse
With $N=$

minutes-days

days-weeks (PC)

weeks-months

10^6 - 10^7

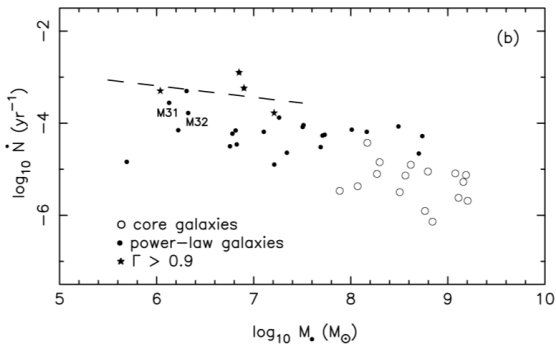
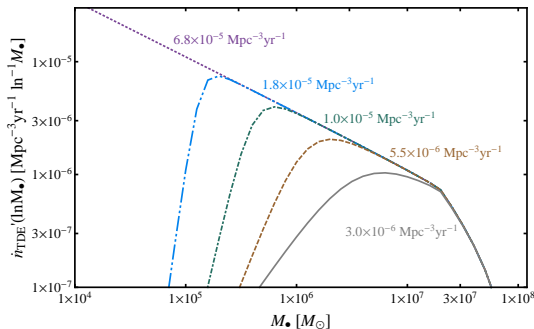
10^5 - 10^6

← **Speed** →
Fast Slow

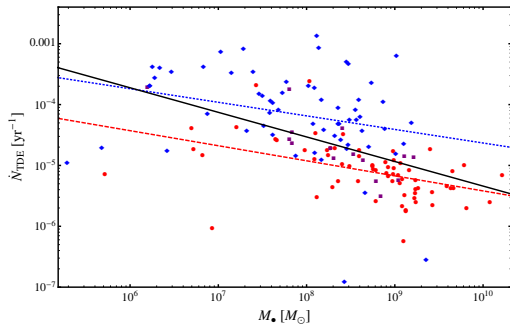
Predicted TDE rates

hover around $10^{-4 \pm 1} \text{ yr}^{-1}$ per galaxy, with a mildly negative trend with M_{\bullet} .

The overall rate is dominated by low-mass black holes, whose demographics are highly uncertain.



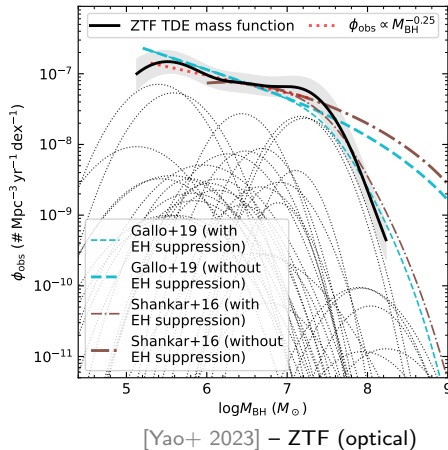
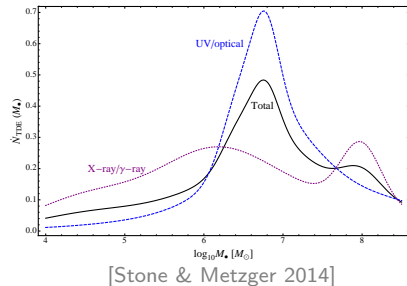
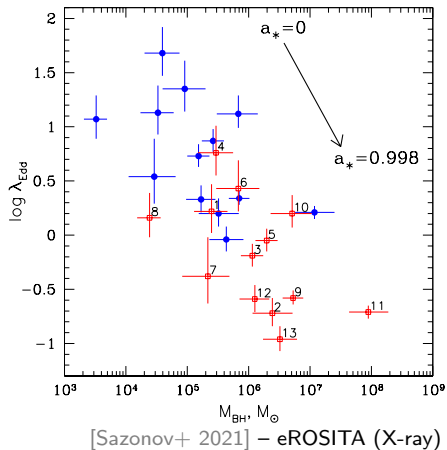
[Wang & Merritt 2004]



[Stone & Metzger 2016]

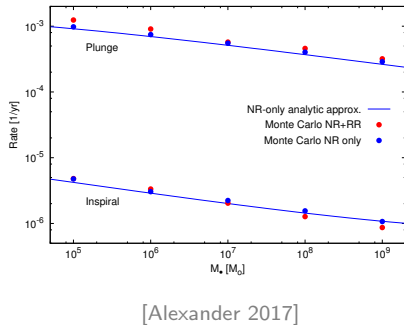
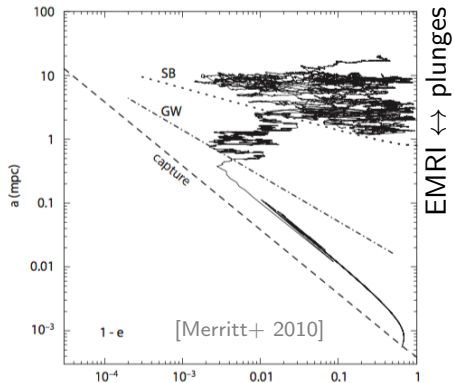
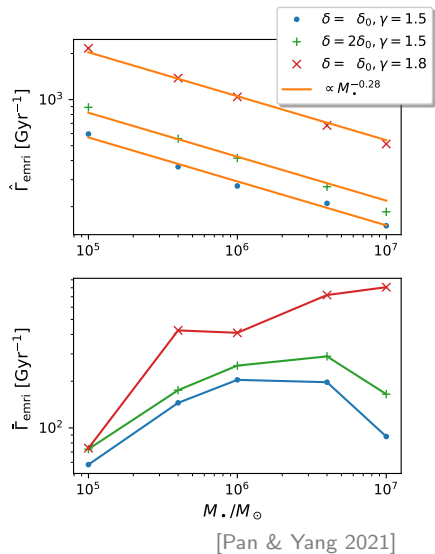
Observed TDE rates

are generally lower by an order of magnitude, though with significant uncertainties about observational selection; in E+A (post-starburst) galaxies the rates are *considerably* higher.



Predicted EMRI rates

are $\sim 10\text{--}100\times$ lower than TDE rates



Observed EMRI rates

[Click here to add content](#)

Observed EMRI rates

Click here to add content (in 15 years)

